

000 001 002 003 004 005 DEEP SPIKING NEURAL NETWORK WITH 006 BRAIN-INSPIRED RECURRENT ITERATIVE LEARNING 007 008 009

010 **Anonymous authors**
011 Paper under double-blind review
012
013
014
015
016
017
018
019
020
021
022
023
024
025
026

ABSTRACT

027 Spiking neural networks (SNNs) have emerged as a transformative paradigm
028 in artificial intelligence, offering event-driven computation and exceptional en-
029 ergy efficiency. However, conventional SNN training methods predominantly
030 rely on backpropagation with surrogate gradients, often neglecting biologically
031 plausible mechanisms such as spike-timing-dependent computations and dynamic
032 excitation-inhibition balance—key features that underpin the brain’s remarkable
033 efficiency and adaptability. To bridge this gap, we propose Brain-Inspired Recur-
034 rent Iterative Learning (BIRIL), a novel hybrid learning framework that synergis-
035 tically integrates biologically realistic spike transmission with adaptive excitation-
036 inhibition dynamics. BIRIL not only emulates the temporal precision of biologi-
037 cal neurons but also dynamically modulates neuronal activity to enhance learning
038 efficiency. Extensive experiments on benchmark datasets—including CIFAR-10,
039 CIFAR-100, MNIST, and DVS128 Gesture—demonstrate that BIRIL outperforms
040 state-of-the-art SNN models, achieving superior accuracy while maintaining low
041 computational overhead. Our work provides a principled approach to advancing
042 neuromorphic learning, paving the way for more brain-like and energy-efficient
043 AI systems.
044

1 INTRODUCTION

045 Artificial Neural Networks (ANNs) have driven transformative progress in machine learning, achiev-
046 ing state-of-the-art performance in domains such as computer vision and natural language pro-
047 cessing. Yet, their reliance on high-precision floating-point computations and global error back-
048 propagation Werbos (1990), diverges fundamentally from the brain’s efficient, event-driven mech-
049 anisms. In contrast, Spiking Neural Networks (SNNs)—the third generation of neural networks
050 Maass (1997)—offer a biologically grounded paradigm, combining event-driven sparsity with ultra-
051 low energy consumption. These properties position SNNs as a compelling alternative to conven-
052 tional ANNs for next-generation AI hardware. However, despite their neuromorphic potential, most
053 deep SNN training methods remain tethered to surrogate gradient backpropagation Wu et al. (2018),
054 mirroring ANN limitations. This approach not only overlooks the critical role of spike-timing-
055 dependent computations but also fails to incorporate dynamic excitation-inhibition balance, a hall-
056 mark of biological learning. Consequently, existing SNNs underutilize their inherent spatiotemporal
057 processing capabilities and face barriers in deploying adaptive on-chip learning for neuromorphic
058 hardware. To bridge this gap, we propose a hybrid learning framework for deep SNNs that syn-
059 ergistically integrates local spike-driven plasticity with global error modulation. By co-optimizing
060 biologically plausible dynamics and task-driven performance, our approach unlocks the full poten-
061 tial of SNNs for efficient, hardware-friendly neuromorphic systems.
062

063 Local and global learning paradigms offer complementary advantages for training SNNs. On one
064 hand, local learning rules, such as spike-timing-dependent plasticity (STDP) Song et al. (2000),
065 closely mimic biological synaptic plasticity by updating weights based on precise temporal rela-
066 tionships between pre- and post-synaptic spikes. These biologically inspired mechanisms enable
067 fully local credit assignment, eliminating dependence on a global loss function while enhancing
068 robustness and hardware compatibility for on-chip learning. On the other hand, global learning
069 methods like spatio-temporal backpropagation (STBP) Wu et al. (2018) leverage surrogate gradi-
070 ents to achieve competitive performance in deep SNNs, albeit at the cost of biological plausibility.
071 While these approaches differ fundamentally, their synergistic integration presents a promising av-
072

054
 055
 056
 057
 058
 059
 060
 061
 062
 063
 064
 065
 066
 067
 068
 069
 070
 071
 072
 073
 074
 075
 076
 077
 078
 079
 080
 081
 082
 083
 084
 085
 086
 087
 088
 089
 090
 091
 092
 093
 094
 095
 096
 097
 098
 099
 100
 101
 102
 103
 104
 105
 106
 107
 enue for developing efficient and versatile SNN training frameworks. Recent work has explored this hybrid approach, such as EICIL Shao et al. (2023), which dynamically combines STDP-based local learning with STBP-driven global updates using an excitation-inhibition gating mechanism. However, while EICIL demonstrates the feasibility of hybrid learning, its performance remains limited in deep SNN architectures, highlighting the need for more scalable and adaptive integration strategies.

Decades of neuroscientific research have revealed that biological neural networks operate through sophisticated synaptic mechanisms Raichle & Mintun (2006), where information is encoded and transmitted via dynamic electro-chemical signal conversion. A fundamental feature of this system is the balanced interplay between excitatory and inhibitory neurons Lauritzen et al. (2012), which modulates downstream neural activity through precisely regulated neurotransmitter release. This delicate excitation-inhibition (E-I) balance is crucial for maintaining stable yet adaptable network dynamics. Therefore, we consider alternating excitation and inhibition during the learning process and designan iterative hybrid global and local learning mechanism in deep SNNs.

In this paper, we propose a novel training framework named Brain-Inspired Recurrent Iterative Learning (BIRIL) for deep SNNs. BIRIL employs a three-cycle training strategy. The strategy comprises an excitation, an inhibition, and an excitation-inhibition mechanism. By mixing these three mechanisms in different proportions, the distribution of excitatory and inhibitory training iterations can be dynamically rebalanced. Hence BIRIL can realistically simulate the excitation/inhibition state of biological neurons, and integrate a parameter update mechanism for both the time and spatial dimension during training. Thus, the BIRIL training framework has better biological interpretability and resembles the real working structure of the human brain.

The contributions of this paper are summarized as follows:

- This paper proposes a novel hybrid training framework based on BIRIL, which enhances the performance of deep SNNs trained with hybrid learning.
- We propose a novel three-cycle training strategy that integrates excitation, inhibition, and the excitation/inhibition mechanism, enhancing the spatiotemporal dynamics of SNNs through the dynamic adjustment of excitatory and inhibitory training iterations.
- Experimental results demonstrate that BIRIL significantly outperforms locally/globally learned SNNs onmultiple benchmark datasets. The results show that theappropriate distribution ratio of BIRIL is quite close to the excitation-inhibition property in the human brain.

2 RELATED WORK

2.1 LEARNING METHODS OF SNNs

Spiking Neural Networks (SNNs) employ two principal learning paradigms: unsupervised local learning and supervised global learning. The first category is exemplified by Spike-Timing-Dependent Plasticity (STDP), a biologically inspired mechanism that adjusts synaptic weights based on temporal correlations between pre- and postsynaptic spikes Song et al. (2000)Nessler et al. (2009). STDP strengthens connections when presynaptic neurons fire before postsynaptic neurons, while weakening them in the reverse temporal order. Recent extensions, such as reward-modulated STDP (R-STDP), incorporate global neuromodulatory signals to enhance learning efficiency Mozafari et al. (2018). However, these biologically plausible approaches often face computational limitations due to their local nature and increased energy demands from reward-processing mechanisms.

The second category addresses supervised learning through adaptations of backpropagation for spiking networks. While conventional backpropagation Werbos (1990) is incompatible with SNNs' discrete spiking dynamics, the Spatio-Temporal Backpropagation (STBP) algorithm overcomes this by employing surrogate gradients to enable differentiable training Wu et al. (2018). STBP effectively captures both spatial and temporal information flow, but its reliance on global error signals and computationally intensive backpropagation through time presents scalability challenges. This fundamental trade-off between biological plausibility and computational efficiency remains a key consideration in SNN learning algorithm design.

108
109

2.2 BRAIN-INSPIRED HYBRID TRAINING

110
111
112
113
114
115
116
117
118
119
120
121
122
123
124

Unlike purely local or global training methods for Spiking Neural Networks (SNNs), hybrid approaches that integrate global Spatio-Temporal Backpropagation (STBP) with local Spike-Timing-Dependent Plasticity (STDP) Yan et al. (2021) provide a more biologically plausible framework by better emulating the spiking dynamics of biological neurons. These methods leverage both STBP and STDP to update synaptic weights, combining the strengths of global gradient-based optimization with local, biologically inspired plasticity rules. For instance, the EICIL method Shao et al. (2023) alternates between STDP and STBP during training, capturing excitatory and inhibitory neuronal behaviors to enhance learning. However, EICIL’s sequential application of STDP and STBP—rather than concurrent optimization—limits its effectiveness, often yielding suboptimal performance. Another approach, Hybrid Plasticity (HP) Wu et al. (2022), separately updates parameters using STBP and STDP before integrating them into the final model. While HP improves accuracy, its dual-parameter optimization introduces significant computational overhead. To address these limitations, we propose an efficient hybrid training method that synergistically combines STDP and STBP, enhancing SNN performance while more faithfully replicating the brain’s biological learning mechanisms.

125

3 PRELIMINARY

126
127
128

3.1 INTEGRATE-AND-FIRE NEURON MODEL

129
130
131
132
133

Integrate-and-Fire (IF) Gerstner et al. (2014) is an important module that simulates the activity of biological neurons in SNNs. IF neurons receive pulse inputs from other neurons and send output pulses to other neurons based on the accumulated charges. As a discrete-time model, IF neurons accumulate each input pulse to generate the membrane potential. If the membrane potential reaches the firing threshold, the neuron outputs a pulse and resets the membrane potential.

134
135
136

At each time step, the membrane potential of an IF neuron accumulates membrane charges from other neurons. The calculation formula of the IF neuron is as follows:

137
138
139

$$V(t) = V(t-1) + \sum_i I_i(t), \quad (1)$$

140
141
142

where $V(t)$ represents the membrane potential at the current time step, $V(t-1)$ represents the membrane potential at the previous time step, and $\sum_i I_i(t)$ represents the input current from the other neuron.

143
144

When the membrane potential exceeds a threshold V_{th} , the IF neuron fires a pulse:

145
146
147

$$S(t) = \begin{cases} 1, & \text{if } V(t) \geq V_{\text{th}}, \\ 0, & \text{if } V(t) < V_{\text{th}}, \end{cases} \quad (2)$$

148
149
150
151

where $S(t)$ represents the spike train, denoting whether the neuron releases a spike at the current time step, and V_{th} is the threshold that triggers the spike release. If the IF neuron fires a spike, it resets the membrane potential.

152
153

3.2 NEURONAL EXCITATION AND INHIBITION

154
155
156
157
158
159
160
161

Neurons in the human brain are connected by synapses, which transmit impulse signals mainly by releasing neurotransmitters. Excitatory neurons and inhibitory neurons produce different effects by releasing different neurotransmitters. The two types of neurons form complex and sophisticated local circuits that play a vital role in regulating the higher brain functions of the cerebral cortex. In different areas of the human brain, the number of excitatory neurons and inhibitory neurons has different ratios. For example, the ratio of excitatory neurons to inhibitory neurons in the cerebral cortex is roughly 4:1. Excitatory neurons promote the strength of synapses through mechanisms such as long-term potentiation (LTP) to strengthen memory. Inhibitory neurons prevent excitatory neurons from overactivity and reduce interference between new information and existing memories,

162 making memory retrieval more explicit. The interaction between neuronal excitatory and inhibitory
 163 properties plays a vital role in the ability of the human brain's nervous system to process information.
 164 Motivated by the above, we think that the training process of SNNs could be adjusted according to
 165 the inhibitory and excitatory distribution.
 166

167 3.3 SPIKE-TIMING-DEPENDENT PLASTICITY(STDP)

168 STDP is widely believed to be a fundamental way of learning and information storage in the human
 169 brain. STDP is attractive because of its excellent biological interpretability. In the human brain,
 170 action potentials often change very precisely according to external stimuli, and STDP simulates this
 171 process very well. Specifically, STDP adjusts the strength of the connection based on the relative
 172 timing of the action potential input and output of a particular neuron. If an input to a neuron occurs
 173 before the output of the neuron, the synapse becomes stronger and becomes a Long-Term Potentiation
 174 (LTP) synapseMalenka & Nicoll (1999), while if an input occurs after the output of the neuron,
 175 the synapse becomes weaker and becomes a Long-Term Depression (LTD) synapseIto (1989).
 176

177 The following equation formulates this process:

$$178 \Delta\omega = \begin{cases} A_+ \cdot e^{-(t_{\text{post}} - t_{\text{pre}})/\tau_+}, & \text{if } t_{\text{post}} > t_{\text{pre}}, \\ 179 A_- \cdot e^{-(t_{\text{pre}} - t_{\text{post}})/\tau_-}, & \text{if } t_{\text{pre}} > t_{\text{post}}, \end{cases} \quad (3)$$

180 where $\Delta\omega$ represents the change in synaptic weight, positive values indicate an increase in weight,
 181 and negative values indicate a decrease in weight, t_{pre} and t_{post} represent the time when the pre-
 182 neuron and post-neuron fire pulses, respectively, A_+ and A_- represent the amplitude of the increase
 183 and decrease in the regulating weight, and changing them can change the strength of synaptic plas-
 184 ticity changes, τ_+ and τ_- are the time constants of weight enhancement and weakening, respectively,
 185 which determine the decay rate of synaptic weight changes.
 186

187 This means that the smaller the time difference between the pulses, the more "important" the synapse
 188 is, and the greater the change in weight is. The larger the time difference between the previous and
 189 next pulses, the more "unimportant" the synapse is, and the smaller the change in weight is. If the
 190 time difference between the two pulses is large enough, the weight of the synapse may not change
 191 significantly.
 192

193 3.4 SPATIO-TEMPORAL BACKPROPAGATION(STBP)

194 Spatio-Temporal Backpropagation is a method that combines the powerful capabilities of the tradi-
 195 tional Backpropagation (BP) algorithm with good biological interpretability.
 196

197 In back propagation, the loss function is formulated as follows:

$$198 L = \frac{1}{2S} \sum_{s=1}^S \|y_s - \frac{1}{T} \sum_{t=1}^T o_s^{t,N}\|_2^2, \quad (4)$$

199 where L is a function of weights and biases, where S is the number of samples in this batch, y_s is
 200 the sample label, $o_s^{t,N}$ is the output at time step t , and the gradient propagates along the time domain
 201 and space domain respectively.
 202

203 Since the discrete spikes in SNNs result in non-differentiable gradients during backpropagation,
 204 alternative gradient functions are required to approximate continuous gradients from the discrete
 205 spike events, known as surrogate gradient methods for SNNs.
 206

207 Among them, the derivative of the sigmoid function is a common and effective gradient substitute
 208 function:
 209

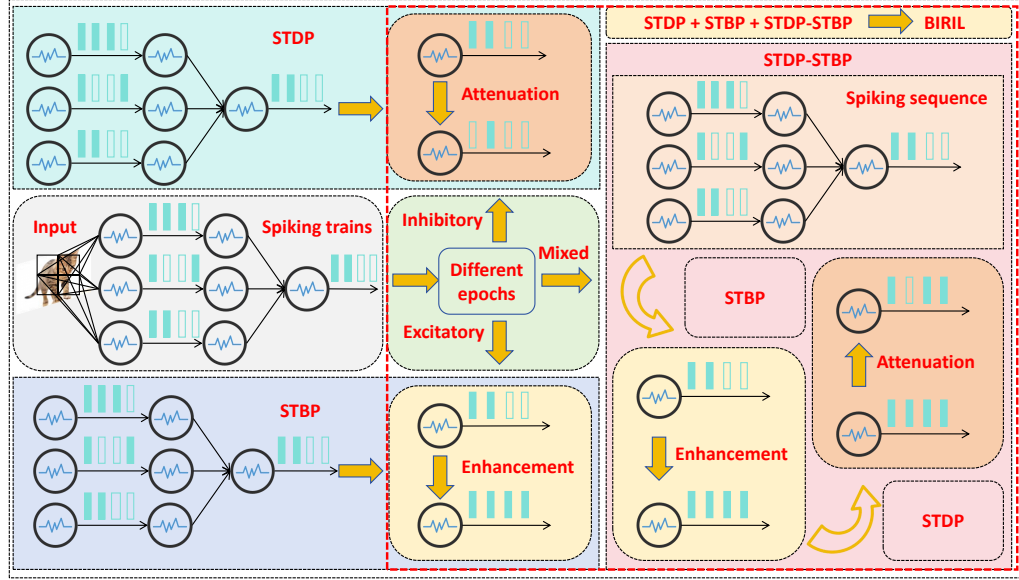
$$210 \text{sigmoid}(x) = \frac{1}{1 + e^{-x}}. \quad (5)$$

211 When solving the derivative of the sigmoid function, we scale it by factor α to make the gradient cal-
 212 culated during backpropagation larger or smaller, thereby effectively accelerating the convergence
 213 process:
 214

$$215 \text{grad}(x) = \alpha \cdot \text{sigmoid}(x) \cdot (1 - \text{sigmoid}(x)). \quad (6)$$

216

217



218

219

220

221

222

223

224

225

226

227

228

229

230

231

232

233

234

235

236

Figure 1: The figure above shows the training model framework, including the backbone network and the residual network, which ensures that the excitation mechanism and the inhibition mechanism can give full play to their respective advantages during training.

237

238

239

240

241

242

243

244

4 METHODS

4.1 MULTI-LAYER STDP

245

246

247

248

249

Due to challenges such as the high computational cost, the nature of neuronal activity, and the complexity of synaptic plasticity mechanisms, traditional STDP is typically applied to a single layer within a neural network, limiting the scope of parameter updates to that specific layer. However, with the advancement of research, multi-layer STDP Vignoud et al. (2018) has gained increasing attention as a means to extend the applicability of STDP to deeper network architectures.

250

251

252

253

254

255

256

257

258

259

To bridge this gap, we propose a hybrid STDP-STBP framework that integrates the biological plausibility of STDP with the global optimization capabilities of STBP. In this framework, STBP is used to update local synaptic weights, while STDP leverages the gradient information from STBP to perform backpropagation. This cyclic gradient update mechanism ensures effective error propagation to earlier layers, addressing the limitations of pure STDP in deep networks. Additionally, we incorporate biologically inspired mechanisms, such as synaptic normalization and spike gating, to further enhance the robustness and efficiency of deep SNN training. By combining the strengths of STDP and STBP, our approach not only preserves the biological principles of human brain learning and feedback but also achieves state-of-the-art performance in deep SNNs without reducing network depth.

260

261

4.2 STDP-STBP GRADIENT UPDATE MECHANISM

262

263

264

265

266

267

268

269

In the learning and memory mechanism of the human brain, there is not only unidirectional pulse transmission but also reverse pulse transmission. The pulse transmission between the neural networks in the human brain is a forward-reverse cycle mode. Previous studies tended to use only one STDP or STBP for unidirectional pulse transmission, which obviously does not conform to the information processing mechanism of the human brain. Therefore, we combined the characteristics of excitatory neurons and inhibitory neurons and the mechanism of neuronal pulse transmission in the human brain and used STDP and STBP to update the weights of neuronal connections. Among them, STDP is used to represent the inhibitory state of neurons, and STBP is used to represent the excitatory state of neurons. Using the different characteristics of STDP and STBP to update the

270 **Algorithm 1** STDP-STBP cyclic gradient update mechanism

271 **Require:** The connection weights between neurons w , Weights updated by STDP Δw_{stdp} ,
 272 Weights updated by STBP Δw_{stbp} ,The time when the front neuron fires a pulse t_{pre} ,The time
 273 when the rear neuron fires a pulse t_{post} .

274 **for** $i = 1$ **to** epoch **do**

275 Neural Network Forward Propagation

276 **if** $t_{pre} < t_{post}$,Presynaptic spike early **then**

277 Use STBP to update the connection weights between neurons in all layers

278 $w \leftarrow w + \Delta w_{stbp}$

279 Next use STDP to update the gradient information of the convolutional layer according to
 Eq. (3)

280 $w \leftarrow w + \Delta w_{stdp}$

281 **else**

282 Same as above, but this time the presynaptic impulse is delayed

283 $w \leftarrow w + \Delta w_{stdp} + \Delta w_{stbp}$

284 **end if**

285 **end for**

gradient information separately can give full play to the performance of the SNN network and make it have better biological interpretability. For STBP, Δw_{ij} represents the change in the connection weight between neuron i and neuron j :

$$\frac{dV_j(t)}{dt} = \sum_{i=1}^N \Delta w_{ij} D(V(t) - s_j(t) \cdot V_{thr}), \quad (7)$$

where $D(\cdot)$ represents the neural model of STBP, $V(t)$ represents the membrane voltage of neuron j , s_i and s_j represent whether the neuron i and neuron j emit pulses respectively, and V_{thr} is the threshold value of the neuron to emit a pulse. Similarly, for STDP, $P(\cdot)$ represents the neural model of STDP, and it is necessary to consider the pulse emission of the front neuron i and the back neuron j at the same time:

$$\frac{dV_j(t)}{dt} = \sum_{i=1}^N \Delta w_{ij} P(V(t) - (s_j(t) + s_i(t)) \cdot V_{thr}). \quad (8)$$

305 In the STDP-STBP cyclic gradient update mechanism, we use STBP to update the connection
306 weights between all neurons including the convolutional layers, and then use STDP to update all
307 convolutional layers in the network to implement a cyclic gradient update mechanism.

308 In the experiment, we also made more attempts, such as using STDP to update the connection
309 weights between neurons in all convolutional layers and fully connected layers in the network and
310 using STBP to update the connection weights between neurons in other layers except convolutional
311 layers and fully connected layers. In this way, STDP and STBP will update the gradients of different
312 layers, reflecting the dynamic combination of neuronal excitability and inhibition.

4.3 BRAIN-INSPIRED RECURRENT ITERATIVE LEARNING

316 In addition to using the STDP-STBP cyclic gradient update mechanism, a certain proportion of
317 STDP and STBP can be added during the training process to update the connection weights between
318 neurons separately. In this way, the excitatory and inhibitory behaviors of neurons can be distin-
319 guished during training, and the problem of gradient information not being able to be updated to
320 earlier layers when using STDP can be effectively avoided.

321 In the human brain, excitatory neurons account for approximately 85%, while inhibitory neurons
322 account for approximately 15%. The fact that excitatory neurons connect to a large number of
323 neurons aligns with the properties of STBP; the fact that inhibitory neurons connect to only a small
number of neurons aligns with the properties of STDP. Therefore, in our model, we use STBP to

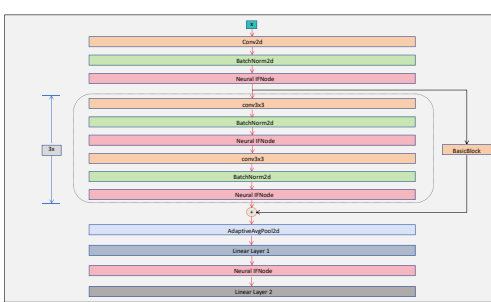


Figure 2: The figure above shows the training model framework, including the backbone network and the residual network, which ensures that the excitation mechanism and the inhibition mechanism can give full play to their respective advantages during training.

represent excitatory neurons and STDP to represent inhibitory neurons. We also use the STDP-STBP cyclic gradient update mechanism to represent excitatory neurons that are closely connected to inhibitory neurons.

In the framework of network model, we use ResNet as the model and build our own network, including convolution layer, normalization layer, activation layer, pooling layer, residual fast and fully connected layer. We use average pooling layers instead of maximum pooling layers to reduce data noise to a certain extent, capture the global information of some features, and make the features smoother. Each residual block contains two sets of convolutional layers, two sets of normalization layers, and two sets of activation layers. For the final output of the model, we expand the single fully connected layer to two sets of fully connected layers plus one set of activation layers, which can effectively extract more advanced features and improve the performance of the model, and can also effectively improve the training effect of STDP.

5 EXPERIMENT

5.1 DATASETS

We evaluate our approach on a workstation equipped with a 16-core Intel(R) Xeon(R) Platinum 8352V CPU and 4 NVIDIA 4090 GPUs. The network architecture used in the experiment is ResNet, and the experimental datasets are: CIFAR-10 Krizhevsky et al. (2010), CIFAR-100 Lin (2013), MNIST Deng (2012), DVS128 Gesture Hu et al. (2022), and Tiny-imagenet Le & Yang (2015).

CIFAR-10 and CIFAR-100 are classic image classification datasets. They are commonly used for the evaluation and comparison of models in the fields of deep learning and computer vision. The MNIST dataset is one of the most well-known datasets in the field of handwritten digit recognition. DVS128 Gesture is a dynamic vision dataset focused on gesture recognition, captured by a dynamic vision sensor. Due to its address-event representation, DVS128 Gesture is very suitable for SNNs.

5.2 EXPERIMENTAL COMPARISON

In this section, we use STDP, STDP-STBP and BIRIL to train our ResNet and compare with other methods. When using STDP training, we use STDP to update the parameters of all convolutional layers in the neural network. STDP-STBP uses STBP to update the parameters of all layers and then uses STDP to update the parameters of the convolutional layer to complete a parameter update loop. BIRIL uses different proportions of STDP, STBP and STDP-STBP for parameter update. In addition, we choose Resnet-18 from STDP-BW-GS Shao et al. (2023) as our base model and draw Figure 3 for comparison. STDP-BW-GS uses STDP to update the parameters of some layers of the neural network, which has certain biological inspiration. Our experimental results are shown in table 1.

378

379

Table 1: Comparison of test accuracy of STDP, STDP-STBP and BIRIL with other methods

380

381

Dataset	STDP (Acc. %)	STDP-STBP(ours) (Acc. %)	BIRIL(ours) (Acc. %)	Improvement (Δ Acc. %)	Baseline Methods (Accuracy Gains)
CIFAR 10	42.23	93.60	93.40	+2.30 +1.06 +4.46	• SSTDP: (91.30% \rightarrow 93.60%) • Diet-SNN: (92.54% \rightarrow 93.60%) • STDP-BW-GS: (89.14% \rightarrow 93.60%)
CIFAR 100	11.54	72.25	70.89	+1.63 +0.56 +18.15	• S-ResNet: (70.62% \rightarrow 72.25%) • STBP-tdBN: (71.69% \rightarrow 72.25%) • STDP-BW-GS: (54.10% \rightarrow 72.25%)
MNIST	89.16	99.26	99.30	+0.40 +0.29 +0.06	• EMSTDP: (98.90% \rightarrow 99.30%) • BPR: (99.01% \rightarrow 99.30%) • STDP-BW-GS: (99.24% \rightarrow 99.30%)
DVS128Gesture	24.31	94.80	95.49	+0.89 +4.97 +8.68	• SNN: (94.60% \rightarrow 95.49%) • R-STDP: (90.52% \rightarrow 95.49%) • STDP-BW-GS: (86.81% \rightarrow 95.49%)

382

323

Note: Improvement (Δ) shows the accuracy gain of STDP-STBP or BIRIL compared with others.

324

325

326

327

328

329

330

331

332

333

334

335

336

337

338

339

340

341

342

343

344

345

346

347

348

349

350

351

352

353

354

355

356

357

358

359

360

361

362

363

364

365

366

367

368

369

370

371

372

373

374

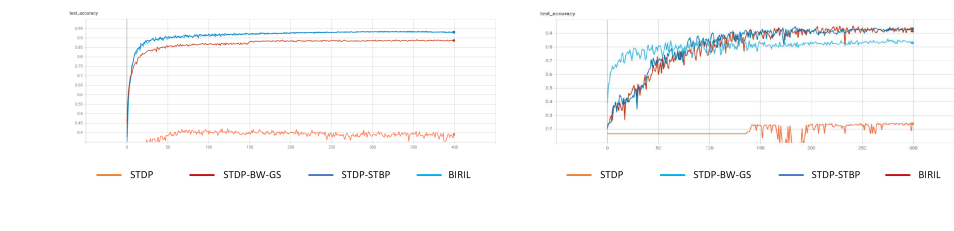
375

376

377

378

379



403

404

405

406

407

408

409

410

411

412

413

414

415

416

417

418

419

420

421

422

423

424

425

426

427

428

429

430

431

432

433

434

435

436

437

438

439

440

441

442

443

444

445

446

447

448

449

450

451

452

453

454

455

456

457

458

459

460

461

462

463

464

465

466

467

468

469

470

471

472

473

474

475

476

477

478

479

480

481

482

483

484

485

486

487

488

489

490

491

492

493

494

495

496

497

498

499

500

501

502

503

504

505

506

507

508

509

510

511

512

513

514

515

516

517

518

519

520

521

522

523

524

525

526

527

528

529

530

531

532

533

534

535

536

537

538

539

540

541

542

543

544

545

546

547

548

549

550

551

552

553

554

555

556

557

558

559

560

561

562

563

564

565

566

567

568

569

570

571

572

573

574

575

576

577

578

579

580

581

582

583

584

585

586

587

588

589

590

591

592

593

594

595

596

597

598

599

600

601

602

603

604

605

606

607

608

609

610

611

612

613

614

615

616

617

618

619

620

621

622

623

624

625

626

627

628

629

630

631

632

633

634

635

636

637

638

639

640

641

432

433

Table 2: Experiments on different ratios between STDP, STBP, and STDP-STBP of BIRIL

434

435

Dataset	Ratio of STDP to STBP to STDP-STBP					Best Ratio
	1:4:1(Acc. %)	1:6:2(Acc. %)	2:6:1(Acc. %)	1:8:3(Acc. %)	3:8:1(Acc. %)	
CIFAR 10	93.21	93.36	93.08	93.40	92.96	1:8:3
CIFAR 100	70.30	70.48	69.70	70.89	69.40	1:8:3
MNIST	99.28	99.30	99.29	99.22	99.23	1:6:2
DVS128Gesture	89.93	88.89	95.49	87.50	89.58	2:6:1

436

437

438

439

440

441

442

443

444

445

446

447

448

449

450

451

Figure 4: Performance of test accuracy of different ratios between STDP, STBP, and STDP-STBP

452

453

454

455

5.3 MIXING RATIO TRAINING OF BIRIL

456

In this section, we examine the impact of different proportions of STDP, STBP, and STDP-STBP cyclic gradient update mechanisms. These different training methods enriched the framework of BIRIL. Through a large number of experiments, we concluded that the optimal ratio of the sum of STDP and STDP-STBP used in the network model to STBP is 1:2. A training framework with this ratio can achieve both excellent performance and good biological interpretability.

457

458

459

460

461

As shown in table 2 and Figure 4, we employ a series of ratios (STDP to STBP to STDP-STBP). On CIFAR-10, the highest accuracy is 93.40%, the lowest is 92.96%, and their difference is 0.44%. On CIFAR-100, the highest accuracy is 70.89%, the lowest is 69.40%, and their difference is 1.49%. The best training ratio on both datasets is 1:8:3, indicating that more inhibitory neurons improve performance. On MNIST, the highest accuracy is 99.30%, the lowest is 99.22%, and their difference is only 0.08%, indicating that BIRIL has a wider range of applicability on smaller datasets. On DVS128 Gesture, the highest accuracy is 95.49%, the lowest is 87.50%, and their difference is 7.99%. The best training ratio is 2:6:1. However, increasing the ratio to 3:8:1 reduces accuracy. This shows that a more excited model is more suitable for this dataset, but an overexcited model reduces the model’s expressiveness. In addition, if the proportion of STDP or STDP-STBP continues to increase unilaterally on the basis of 1:8:3 or 3:8:1, the network will gradually enter an over-excited or over-inhibited state, which is not conducive to the training results. The different ratios of STDP, STBP, and STDP-STBP make the BIRIL framework both flexible and biologically interpretable. Different ratios can construct BIRIL with different degrees of excitation/inhibition. We can build the most adaptable framework in a targeted manner on different datasets, which greatly enhances the versatility of our model.

477

478

479

6 CONCLUSION

480

481

482

483

484

485

By simulating the excitatory and inhibitory mechanisms of neurons in the human brain, our proposed Bidirectional Inhibitory and Regulatory Integrative Learning (BIRIL) model significantly enhances the performance of Spiking Neural Networks (SNNs). Experimental results demonstrate that the BIRIL model exhibits strong expressiveness, superior biological interpretability, and robust generalization capabilities across both small- and large-scale datasets. In future work, we aim to further investigate the dynamic balance between excitation and inhibition in biological neural systems.

486 REFERENCES
487

488 Arnon Amir, Brian Taba, David Berg, Timothy Melano, Jeffrey McKinstry, Carmelo Di Nolfo,
489 Tapan Nayak, Alexander Andreopoulos, Guillaume Garreau, Marcela Mendoza, et al. A low
490 power, fully event-based gesture recognition system. In *Proceedings of the IEEE conference on*
491 *computer vision and pattern recognition*, pp. 7243–7252, 2017.

492 Li Deng. The mnist database of handwritten digit images for machine learning research [best of the
493 web]. *IEEE signal processing magazine*, 29(6):141–142, 2012.

494 Wulfram Gerstner, Werner M Kistler, Richard Naud, and Liam Paninski. *Neuronal dynamics: From*
495 *single neurons to networks and models of cognition*. Cambridge University Press, 2014.

496 Yangfan Hu, Huajin Tang, and Gang Pan. Spiking deep residual networks. *IEEE Transactions on*
497 *Neural Networks and Learning Systems*, 34(8):5200–5205, 2021.

498 Yu Hu, Ziteng Li, Xinpeng Li, Jianfeng Li, Xintong Yu, Xiaofan Chen, and Lei Wang. Hand gesture
499 recognition system using the dynamic vision sensor. In *2022 5th International Conference on*
500 *Circuits, Systems and Simulation (ICCSS)*, pp. 102–110. IEEE, 2022.

501 Masao Ito. Long-term depression. *Annual review of neuroscience*, 12:85–102, 1989.

502 Alex Krizhevsky, Geoff Hinton, et al. Convolutional deep belief networks on cifar-10. *Unpublished*
503 *manuscript*, 40(7):1–9, 2010.

504 Martin Lauritzen, Claus Mathiesen, Katharina Schaefer, and Kirsten J Thomsen. Neuronal inhi-
505 bition and excitation, and the dichotomic control of brain hemodynamic and oxygen responses.
506 *Neuroimage*, 62(2):1040–1050, 2012.

507 Ya Le and Xuan Yang. Tiny imagenet visual recognition challenge. *CS 231N*, 7(7):3, 2015.

508 M Lin. Network in network. *arXiv preprint arXiv:1312.4400*, 2013.

509 Fangxin Liu, Wenbo Zhao, Yongbiao Chen, Zongwu Wang, Tao Yang, and Li Jiang. Sstdp: Super-
510 *vised spike timing dependent plasticity for efficient spiking neural network training*. *Frontiers in*
511 *Neuroscience*, 15:756876, 2021.

512 Wolfgang Maass. Networks of spiking neurons: the third generation of neural network models.
513 *Neural networks*, 10(9):1659–1671, 1997.

514 Robert C Malenka and Roger A Nicoll. Long-term potentiation—a decade of progress? *Science*, 285
515 (5435):1870–1874, 1999.

516 Milad Mozafari, Saeed Reza Kheradpisheh, Timothée Masquelier, Abbas Nowzari-Dalini, and Mo-
517 hammad Ganjtabesh. First-spike-based visual categorization using reward-modulated stdp. *IEEE*
518 *transactions on neural networks and learning systems*, 29(12):6178–6190, 2018.

519 Alireza Nadafian, Milad Mozafari, Timothée Masquelier, and Mohammad Ganjtabesh. Brain-
520 inspired computational modeling of action recognition with recurrent spiking neural networks
521 equipped with reinforcement delay learning. *arXiv preprint arXiv:2406.11778*, 2024.

522 Bernhard Nessler, Michael Pfeiffer, and Wolfgang Maass. Stdp enables spiking neurons to detect
523 hidden causes of their inputs. *Advances in neural information processing systems*, 22, 2009.

524 Marcus E Raichle and Mark A Mintun. Brain work and brain imaging. *Annu. Rev. Neurosci.*, 29(1):
525 449–476, 2006.

526 Nitin Rathi and Kaushik Roy. Diet-snn: A low-latency spiking neural network with direct input
527 encoding and leakage and threshold optimization. *IEEE Transactions on Neural Networks and*
528 *Learning Systems*, 34(6):3174–3182, 2021.

529 Zihang Shao, Xuanye Fang, Yixin Li, Chaoran Feng, Jiangrong Shen, and Qi Xu. Eicil: joint
530 excitatory inhibitory cycle iteration learning for deep spiking neural networks. *Advances in Neural*
531 *Information Processing Systems*, 36:32117–32128, 2023.

540 Amar Shrestha, Haowen Fang, Daniel Patrick Rider, Zaidao Mei, and Qinru Qiu. In-hardware learn-
 541 ing of multilayer spiking neural networks on a neuromorphic processor. In *2021 58th ACM/IEEE*
 542 *Design Automation Conference (DAC)*, pp. 367–372. IEEE, 2021.

543

544 Sen Song, Kenneth D Miller, and Larry F Abbott. Competitive hebbian learning through spike-
 545 timing-dependent synaptic plasticity. *Nature neuroscience*, 3(9):919–926, 2000.

546 Gaëtan Vignoud, Laurent Venance, and Jonathan D Touboul. Interplay of multiple pathways and
 547 activity-dependent rules in stdp. *PLoS computational biology*, 14(8):e1006184, 2018.

548

549 Paul J Werbos. Backpropagation through time: what it does and how to do it. *Proceedings of the*
 550 *IEEE*, 78(10):1550–1560, 1990.

551

552 Yujie Wu, Lei Deng, Guoqi Li, Jun Zhu, and Luping Shi. Spatio-temporal backpropagation for
 553 training high-performance spiking neural networks. *Frontiers in neuroscience*, 12:331, 2018.

554

555 Yujie Wu, Rong Zhao, Jun Zhu, Feng Chen, Mingkun Xu, Guoqi Li, Sen Song, Lei Deng, Guanrui
 556 Wang, Hao Zheng, et al. Brain-inspired global-local learning incorporated with neuromorphic
 557 computing. *Nature Communications*, 13(1):65, 2022.

558

559 Yulong Yan, Haoming Chu, Xin Chen, Yi Jin, Yuxiang Huan, Lirong Zheng, and Zhuo Zou. Graph-
 560 based spatio-temporal backpropagation for training spiking neural networks. In *2021 IEEE 3rd*
561 International Conference on Artificial Intelligence Circuits and Systems (AICAS), pp. 1–4. IEEE,
 562 2021.

563

564 Tielin Zhang, Shuncheng Jia, Xiang Cheng, and Bo Xu. Tuning convolutional spiking neural net-
 565 work with biologically plausible reward propagation. *IEEE Transactions on Neural Networks and*
566 Learning Systems, 33(12):7621–7631, 2021.

567

568 Hanle Zheng, Yujie Wu, Lei Deng, Yifan Hu, and Guoqi Li. Going deeper with directly-trained
 569 larger spiking neural networks. In *Proceedings of the AAAI conference on artificial intelligence*,
 570 volume 35, pp. 11062–11070, 2021.

571

572 A APPENDIX

573 A.1 USE OF LLMs

574 Large Language Models (LLMs) were used solely to assist with polishing the text.

575 A.2 CODE OF ETHICS AND ETHICS STATEMENT

576 The research conducted in the paper conform, in every respect, with the ICLR Code of Ethics
 577 <https://iclr.cc/public/CodeOfEthics>.